

**POSSIBLE DIFFERENCE BETWEEN MULTIPLICITY DISTRIBUTIONS
AND INCLUSIVE SPECTRA OF SECONDARY HADRONS IN
PROTON-PROTON AND PROTON-ANTIPROTON COLLISIONS AT
ENERGY $\sqrt{s} = 900$ GeV**

V.A. Abramovsky[†], N.V. Radchenko[‡]

Novgorod State University

[†] *E-mail: Victor.Abramovsky@novsu.ru*

[‡] *E-mail: nvrad@mail.ru*

Abstract

We consider QCD based model of hadrons interaction in which gluons density in wave function of initial state is low in rapidity space and real hadrons are produced by decay of color field strings. Hadrons production processes in pp and $p\bar{p}$ interactions differ on principle. There are three types of inelastic processes in $p\bar{p}$ collision. The first type is production of secondary hadrons shower from decay of gluon string. The second type is shower produced from decay of two quark strings and the third one – from decay of three quark strings. At the same time there are only two types of inelastic processes for pp collision, they are shower from gluon string and shower from two quark strings. Therefore multiplicity distributions and inclusive spectra of secondary hadrons are different in pp and $p\bar{p}$ interactions, and this difference may be observed at energy $\sqrt{s} = 900$ GeV.

1 Introduction

The measurements of the properties of proton-proton collisions at Large Hadron Collider (LHC) at a center-of-mass energy $\sqrt{s} = 900$ GeV may lead to discovery of “new physics” in soft interactions at high energies. There are sufficiently precise data for proton-antiproton collisions at the same energy including charged particle multiplicity distributions P_n and pseudorapidity distributions $dN_{ch}/d\eta$ [1, 2]. The comparison of these values with forthcoming measurements of LHC will give the opportunity to find out whether multiple characteristics are the same in pp and $p\bar{p}$ interactions.

The data obtained by ALICE coll. on 23rd November 2009 at $\sqrt{s} = 900$ GeV [3] do not allow to make definite conclusions because of large uncertainties.

In this article we argue that there are differences in multiple production in pp and $p\bar{p}$ interactions. These differences may be observed at $\sqrt{s} = 900$ GeV. We give predictions for absolute value of inclusive cross section $d\sigma^{incl}/d\eta$ in Fig. 1 and absolute value of inclusive cross section $d\sigma_n^{incl}/d\eta$ for interval of charged multiplicity $62 \leq n \leq 70$ in Fig. 2 (all cross sections are in millibarns). Detailed discussion of these results is in the following sections.

This article is organized as follows: Section 2 describes the details of our model; elementary inelastic subprocesses are described in Section 3; Section 4 is dedicated to inclusive pseudorapidity distributions and discussion of results.

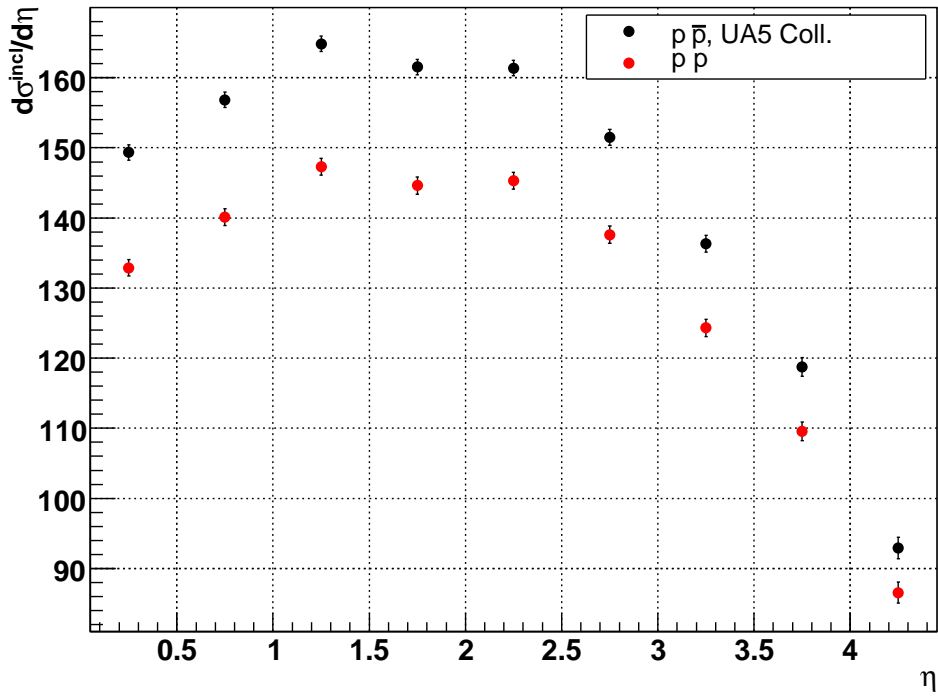


Figure 1: Absolute value of inclusive cross section at $\sqrt{s} = 900$ GeV

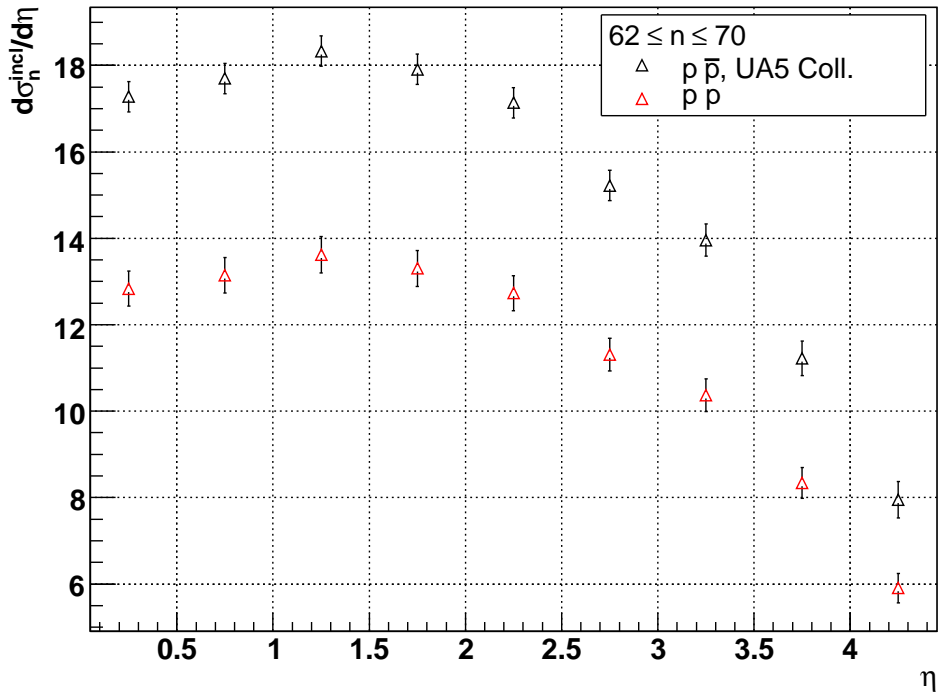


Figure 2: Absolute value of inclusive cross section for charged multiplicity interval $62 \leq n \leq 70$ at $\sqrt{s} = 900$ GeV

2 Low Constituents Number Model

It is generally agreed that the same elementary subprocesses contribute to hadrons production in pp and $p\bar{p}$ interactions at high energies, they are “pomeron showers” [4]. These showers correspond to cuts of different numbers of pomerons, their relations are defined by Abramovsky-Gribov-Kancheli theorem [5]. Contributions of non vacuum reggeons die out at high energies. Therefore it is considered that multiple production characteristics such as charged particle multiplicity distributions and inclusive spectra are the same in pp and $p\bar{p}$ collisions. This idea is used in number of papers, for example [6, 7].

We emphasize that inelastic processes that contribute to pp and $p\bar{p}$ interactions are different and have nothing in common with picture of multiple pomeron showers (now they are called multiple parton interactions). The difference is connected to the fact that two “elementary” inelastic subprocesses contribute to inelastic production in pp scattering and three “elementary” inelastic subprocesses – in $p\bar{p}$ scattering [8] – [12].

We explain physics of this phenomenon on the base of Low Constituents Number Model (LCNM) [13]. It is QCD based model of hadrons interaction in which gluons density in wave function of initial state is low in rapidity space and real hadrons are produced by decay of color field strings. The main features of this model are the following.

- Sizes R of hadrons consisting of light quarks are large, value of coupling constant $\alpha_s(R)$ is large and it is in region of strong coupling. Therefore there are strong color fields of non perturbative nature inside hadron. Fragmentation region of structure function of hadron is filled only with valence quarks, because transverse gluons have sense only in region of weak coupling, where the value of coupling constant $\alpha_s(r_g)$ is small; here r_g – characteristic sizes for which transverse real gluons do not overlap with light quarks. These transverse gluons occur in central region of structure function of fast hadron as “bremsstrahlung” gluons. Since value of $\alpha_s(r_g)$ is small then number of bremsstrahlung transverse gluons is small, i.e. their spectrum is sparse.
- Initial state of hadrons at high energies corresponds to thin disks with thickness of $1/\sqrt{s}$ with strong color fields concentrated inside them. When disks get over each other instantaneous Coulomb exchange takes place and color charge exchange occurs. Then these thin disks move apart and color strings stretch between them¹.

3 Elementary inelastic subprocesses in pp and $p\bar{p}$ interactions

Based on these assumptions we supposed in [8, 9] that interaction between hadrons is carried out by color exchange of only one gluon, and there are only one and two additional bremsstrahlung transverse gluons in initial state of colliding hadrons beside valence quarks.

We formalize our treating by introducing diagrams for elementary subprocesses for $p\bar{p}$ and pp collisions, Fig. 3, 4. Solid lines correspond to quarks and antiquarks, wavy lines to gluons, spirals to strings. Interaction in final state is marked by dotted block.

The diagram in Fig. 3a describes process of $p\bar{p}$ interaction in case when only valence quarks and antiquarks are in initial state. This diagram gives constant part of $p\bar{p}$ total cross section. Interaction occurs as result of gluon exchange between colorless states. Thereat colorless

¹As color field string we define tube of color field with transverse size much less than linear size.

states (proton and antiproton) gain octet color charges and move apart. Color field string is produced between them and when length of string becomes large it decays into secondary hadrons.

Process of $p\bar{p}$ interaction in case when there are valence quarks and one additional bremsstrahlung transverse gluon in initial state is shown in diagram in Fig. 3b. One of quark strings in final state absorbs additional gluon and changes color charge². Contribution from diagram in Fig. 3b to total cross section increases with energy proportionally to $\ln s$.

Processes of $p\bar{p}$ interaction in case when there are valence quarks and two additional bremsstrahlung transverse gluons in initial state are shown in diagrams in Fig. 3c and 3d. In diagram in Fig. 3c both gluons are absorbed by the same quark string. It can be argued [9, 12] that in such case there are two quark strings in final state. In diagram in Fig. 3d gluons are absorbed by different strings. From the same reasons [9, 12] there are three quark strings in final state. Contributions from diagrams in Fig. 3c and 3d to total cross section increase with energy proportionally to $\ln^2 s$.

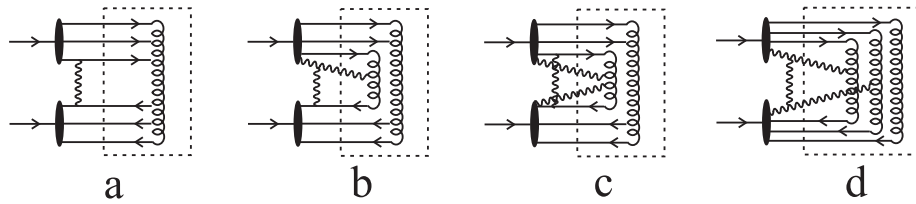


Figure 3: Types of inelastic subprocesses for $p\bar{p}$

Elementary processes of pp interaction we describe by diagrams in Fig. 4.

Process of pp interaction in case when only valence quarks are in initial state is shown in Fig. 4a. This diagram gives constant part of pp total cross section, its contribution completely coincides with contribution from the corresponding diagram of $p\bar{p}$ in Fig. 3a.

Diagrams in Fig. 4b and 4c describe hadrons production process in two quark strings for one and two additional gluons correspondingly. Gluons are absorbed by one and two color strings which change color charge. Contribution from diagram in Fig. 4b to total cross section is proportional to $\ln s$ and coincides with contribution from diagram in Fig. 3b. Contribution from diagram in Fig. 4c to total cross section is proportional to $\ln^2 s$.

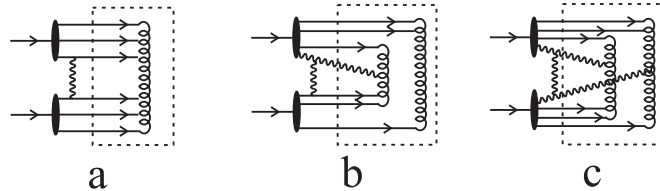


Figure 4: Types of inelastic subprocesses for pp

In this way in pp interaction quark strings arise between quark of one proton and diquark of another one therefore state with more than two quark strings is impossible. At the same time in $p\bar{p}$ interaction quark strings can be produced between every quark of proton and antiquark of antiproton. So in this case state with three quark strings is possible.

This effect defines difference in multiple characteristics of pp and $p\bar{p}$ interactions.

²Dynamics of color leading to change of color charge of quark string will be published later.

4 Inclusive pseudorapidity distributions in pp and $p\bar{p}$ interactions

In every individual event n charged and m neutral particles are produced. We do not distinguish sign of charge so we consider all charged particles as identical and all neutral particles as identical. Topological cross section of production of n charged and m neutral particles is defined as

$$\sigma_{n+m} = \frac{1}{n!m!} \int d\tau_{n+m} \left| A_{2 \rightarrow n+m}(\vec{p}_1, \dots, \vec{p}_n, \vec{q}_{n+1}, \dots, \vec{q}_{n+m}) \right|^2, \quad (1)$$

where $A_{2 \rightarrow n+m}(\vec{p}_1, \dots, \vec{p}_n, \vec{q}_{n+1}, \dots, \vec{q}_{n+m})$ – amplitude of production of n charged and m neutral particles with corresponding momenta \vec{p}_i, \vec{q}_j ; $d\tau_{n+m}$ – corresponding phase volume. Topological cross section of production of n charged particles is defined as

$$\sigma_n = \sum_{m=0}^{\infty} \sigma_{n+m} = \frac{1}{n!} \sum_{m=0}^{\infty} \frac{1}{m!} \int d\tau_{n+m} \left| A_{2 \rightarrow n+m}(\vec{p}_1, \dots, \vec{p}_n, \vec{q}_{n+1}, \dots, \vec{q}_{n+m}) \right|^2. \quad (2)$$

Invariant inclusive cross section of production of one charged particle in event with n charged particles can be defined as following:

$$(2\pi)^3 2E_1 \frac{d^3\sigma_n^{incl}}{d^3p_1} = \frac{1}{(n-1)!} \sum_{m=0}^{\infty} \frac{1}{m!} \int d\tau_{n-1+m} \left| A_{2 \rightarrow n+m}(\vec{p}_1; \vec{p}_2, \dots, \vec{p}_n, \vec{q}_{n+1}, \dots, \vec{q}_{n+m}) \right|^2, \quad (3)$$

where integration in $d\tau_{n-1+m}$ is performed by all momenta starting from \vec{p}_2, \dots

Invariant inclusive cross section can be written as:

$$(2\pi)^3 2E_1 \frac{d^3\sigma^{incl}}{d^3p_1} = \sum_{n=1}^{\infty} (2\pi)^3 2E_1 \frac{d^3\sigma_n^{incl}}{d^3p_1}. \quad (4)$$

Inclusive cross section is normalized by mean multiplicity of corresponding cross section of inelastic process, here we use non single diffraction cross section σ^{nsd} .

$$\int d^3p_1 \frac{d^3\sigma^{incl}}{d^3p_1} = \langle n \rangle \sigma^{nsd} \quad (5)$$

At the same time cross section $d^3\sigma_n^{incl}/d^3p_1$ is normalized by the following relation:

$$\int d^3p_1 \frac{d^3\sigma_n^{incl}}{d^3p_1} = n \sigma_n. \quad (6)$$

where n – number of charged particles in event and σ_n – corresponding topological cross section defined by (2).

We can obtain expressions for inclusive cross sections $d\sigma^{incl}/d\eta$ for pseudorapidity η (or $d\sigma^{incl}/dy$ for rapidity y) by using integral of (3) and (4) of transverse components of momentum \vec{p}_1 .

Normalization of these cross sections is obvious.

$$\int d\eta \frac{d\sigma^{incl}}{d\eta} = \langle n \rangle \sigma^{nsd} \quad (7)$$

$$\int d\eta \frac{d\sigma_n^{incl}}{d\eta} = n \sigma_n \quad (8)$$

We can rewrite (8) as

$$\frac{1}{\sigma^{nsd}} \int d\eta \frac{d\sigma_n^{incl}}{d\eta} = n \frac{\sigma_n}{\sigma^{nsd}} = n P_n. \quad (9)$$

We think that inclusive cross sections $d\sigma^{incl}/d\eta$ ($d\sigma^{incl}/dy$) are the most informative. Unfortunately, we did not find such experimental data for pp and $p\bar{p}$ interactions. However, UA5 Collaboration gave data on inclusive cross sections in nine bins depending on number of charged particles ($2 \leq n \leq 10$, $12 \leq n \leq 20$, \dots , $n \geq 82$).

We define the following notations:

$$\sigma^{(1)} = \sum_{n=2}^{10} \sigma_n, \quad \sigma^{(2)} = \sum_{n=12}^{20} \sigma_n, \quad \dots \quad \sigma^{(9)} = \sum_{n=82}^{\infty} \sigma_n, \quad (10)$$

$$\sum_{i=1}^9 \sigma^{(i)} = \sigma^{nsd}. \quad (11)$$

Also we define

$$\frac{d\sigma^{(1)incl}}{d\eta} = \sum_{n=2}^{10} \frac{d\sigma_n^{incl}}{d\eta}, \quad \dots \quad \frac{d\sigma^{(9)incl}}{d\eta} = \sum_{n=82}^{\infty} \frac{d\sigma_n^{incl}}{d\eta}, \quad (12)$$

$$\sum_{i=1}^9 \frac{d\sigma^{(i)incl}}{d\eta} = \frac{d\sigma^{incl}}{d\eta}. \quad (13)$$

Data of UA5 Collaboration are given in format

$$\frac{1}{\sigma^{(i)}} \frac{d\sigma^{(i)incl}}{d\eta}. \quad (14)$$

We integrated the expression $\frac{1}{\sigma^{nsd}} \frac{d\sigma^{(i)incl}}{d\eta}$ over pseudorapidity space using (8) and obtained

$$\frac{1}{\sigma^{nsd}} \int d\eta \frac{d\sigma^{(i)incl}}{d\eta} = \frac{1}{\sigma^{nsd}} \sum_{n \text{ in bin}} \int d\eta \frac{d\sigma_n^{incl}}{d\eta} = \sum_{n \text{ in bin}} n \frac{\sigma_n}{\sigma^{nsd}} = \sum_{n \text{ in bin}} n P_n = \bar{n}^{(i)}, \quad (15)$$

where $\bar{n}^{(i)}$ is defined as

$$\bar{n}^{(1)} = \sum_{n=2}^{10} n P_n, \quad \bar{n}^{(2)} = \sum_{n=12}^{20} n P_n, \quad \dots \quad \bar{n}^{(9)} = \sum_{n=82}^{\infty} n P_n.$$

Non single diffraction cross sections are the same for pp and $p\bar{p}$ interactions because of Pomeranchuk theorem. But shapes of multiplicity distribution curves are different for pp and $p\bar{p}$ since underlying elementary subprocesses are different (see Section 3 and Fig. 5). Therefore values of $\bar{n}^{(i)}$ are different for pp and $p\bar{p}$ collisions, we denote them $\bar{n}_{pp}^{(i)}$ and $\bar{n}_{p\bar{p}}^{(i)}$ correspondingly.

From relation (15) it follows

$$\int d\eta \frac{d\sigma_{pp}^{(i)incl}}{d\eta} / \int d\eta \frac{d\sigma_{p\bar{p}}^{(i)incl}}{d\eta} = \frac{\bar{n}_{pp}^{(i)}}{\bar{n}_{p\bar{p}}^{(i)}}. \quad (16)$$

The expression $\bar{n}_{pp}^{(i)}/\bar{n}_{p\bar{p}}^{(i)}$ does not depend on pseudorapidity. Besides, number of charged particles in each bin can be taken arbitrary but relation (16) is kept strictly. Therefore we have for inclusive cross sections

$$\frac{d\sigma_{pp}^{(i)incl}}{d\eta} \bigg/ \frac{d\sigma_{p\bar{p}}^{(i)incl}}{d\eta} = \frac{\bar{n}_{pp}^{(i)}}{\bar{n}_{p\bar{p}}^{(i)}}. \quad (17)$$

From here

$$\frac{d\sigma_{pp}^{(i)incl}}{d\eta} = \frac{\bar{n}_{pp}^{(i)}}{\bar{n}_{p\bar{p}}^{(i)}} \frac{d\sigma_{p\bar{p}}^{(i)incl}}{d\eta}. \quad (18)$$

From LCNM and fitting of multiplicity distributions for pp and $p\bar{p}$ at different energies [9, 11] we obtained prediction for multiplicity distribution in pp scattering at $\sqrt{s} = 900$ GeV, Fig. 5.

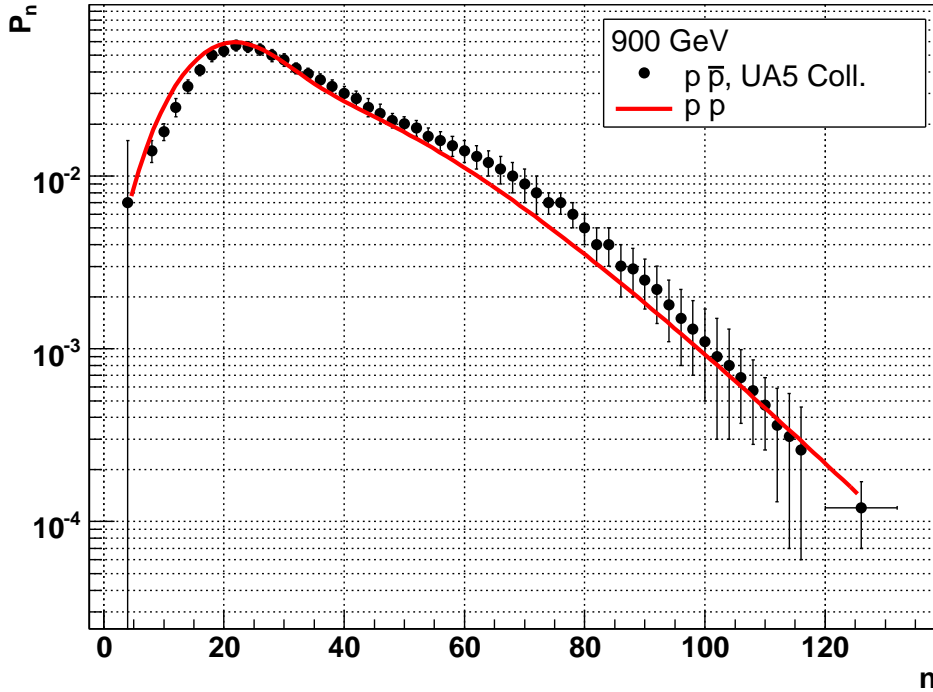


Figure 5: Multiplicity distribution for $p\bar{p}$ at $\sqrt{s} = 900$ GeV (points) and prediction for pp at the same energy in LCNM (red line)

Table 1: Coefficient for inclusive pseudorapidity distributions

	$2 \leq n \leq 10$	$12 \leq n \leq 20$	$22 \leq n \leq 30$	$32 \leq n \leq 40$	$42 \leq n \leq 50$
$\bar{n}_{pp}^{(i)}/\bar{n}_{p\bar{p}}^{(i)}$	1.31 ± 0.01	1.16 ± 0.01	1.01 ± 0.01	0.92 ± 0.01	0.91 ± 0.01
	$52 \leq n \leq 60$	$62 \leq n \leq 70$	$72 \leq n \leq 80$	$n \geq 82$	
$\bar{n}_{pp}^{(i)}/\bar{n}_{p\bar{p}}^{(i)}$	0.85 ± 0.01	0.74 ± 0.02	0.69 ± 0.01	0.79 ± 0.02	

We calculated the values of coefficients $\bar{n}_{pp}^{(i)}/\bar{n}_{p\bar{p}}^{(i)}$ for nine bins of multiplicity to estimate the difference in inclusive cross sections for pp and $p\bar{p}$ with (18), Table 1. Values of probabilities

P_n for pp we took from our prediction in case when 75% of two gluons give three quark strings in $p\bar{p}$, values of P_n for $p\bar{p}$ we took from UA5 experiment [1]. Inclusive pseudorapidity distributions for all bins of charged multiplicity are shown in Fig. 6-13 and Fig. 2. From (13) we obtained the absolute value of inclusive pseudorapidity distribution, shown in Fig. 1.

Quite obviously that inclusive distribution give less visible difference than inclusive distributions in different bins. This is due to fact that multiplicity distribution for pp has higher values before peak and in peak, but lower values in tail of distribution than for $p\bar{p}$. So difference is compensated in sum.

In conclusion we want to stress that difference between pp and $p\bar{p}$ interactions may be observed even at energy $\sqrt{s} = 900$ GeV, especially in inclusive distributions in different bins of charged multiplicity.

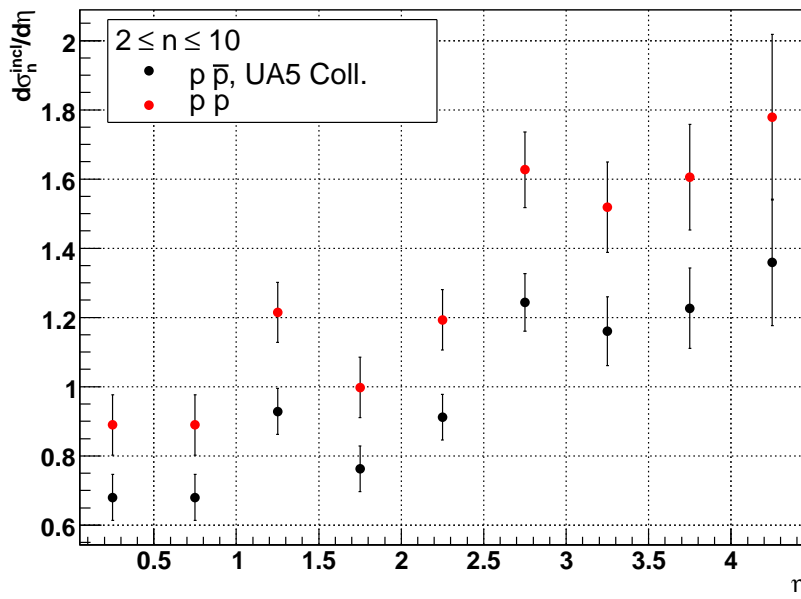


Figure 6: Inclusive pseudorapidity distributions for $2 \leq n \leq 10$

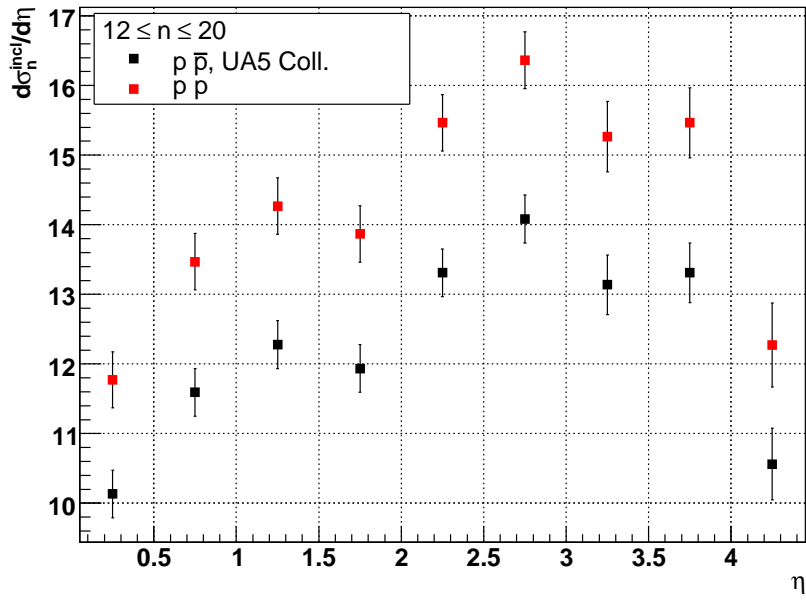


Figure 7: Inclusive pseudorapidity distributions for $12 \leq n \leq 20$

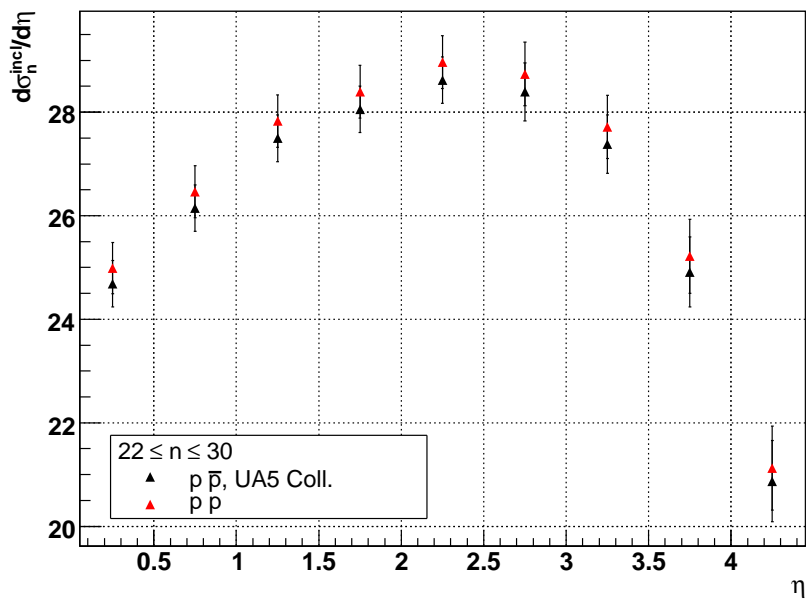


Figure 8: Inclusive pseudorapidity distributions for $22 \leq n \leq 30$

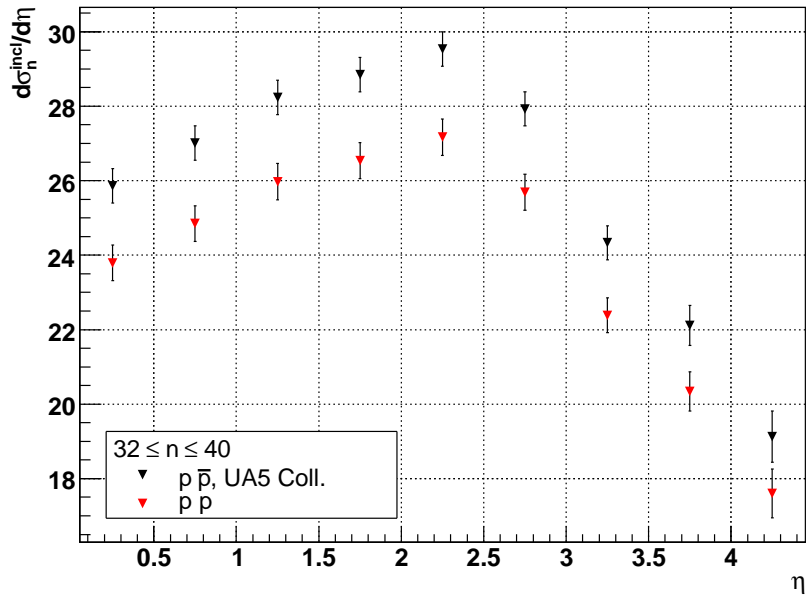


Figure 9: Inclusive pseudorapidity distributions for $32 \leq n \leq 40$

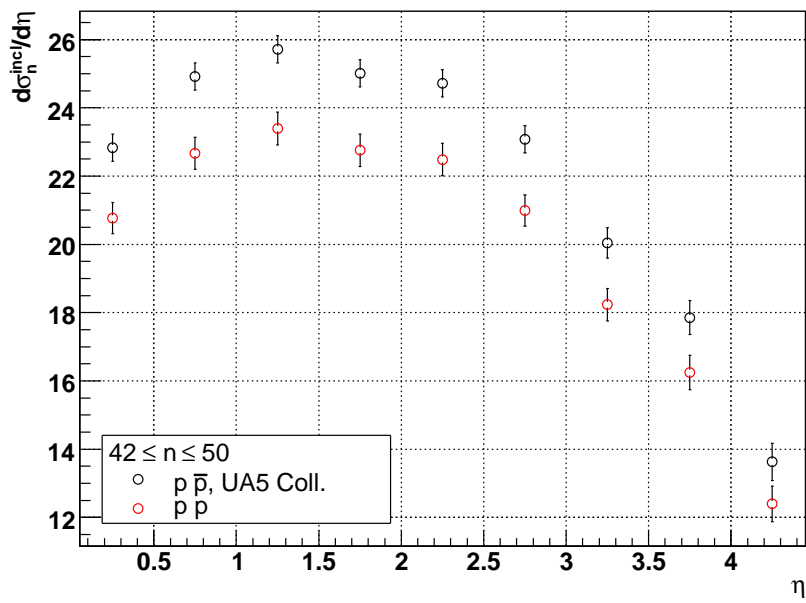


Figure 10: Inclusive pseudorapidity distributions for $42 \leq n \leq 50$

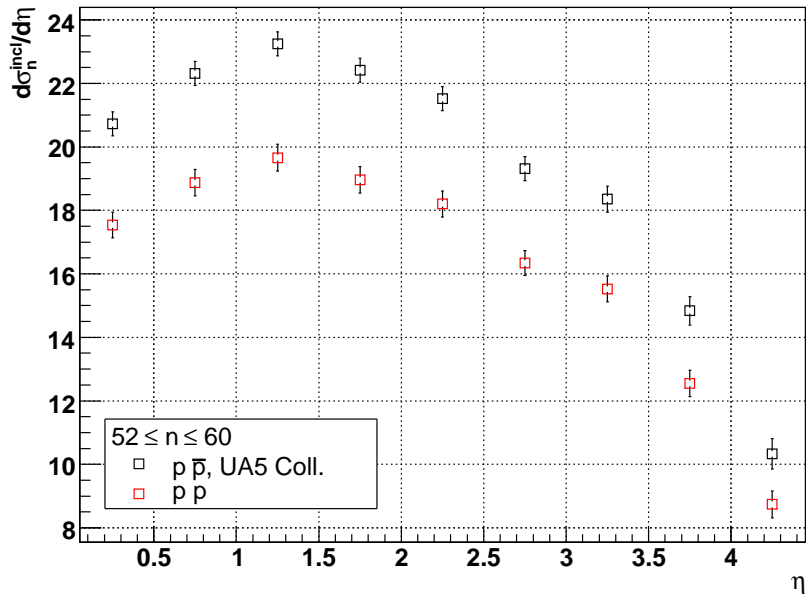


Figure 11: Inclusive pseudorapidity distributions for $52 \leq n \leq 60$

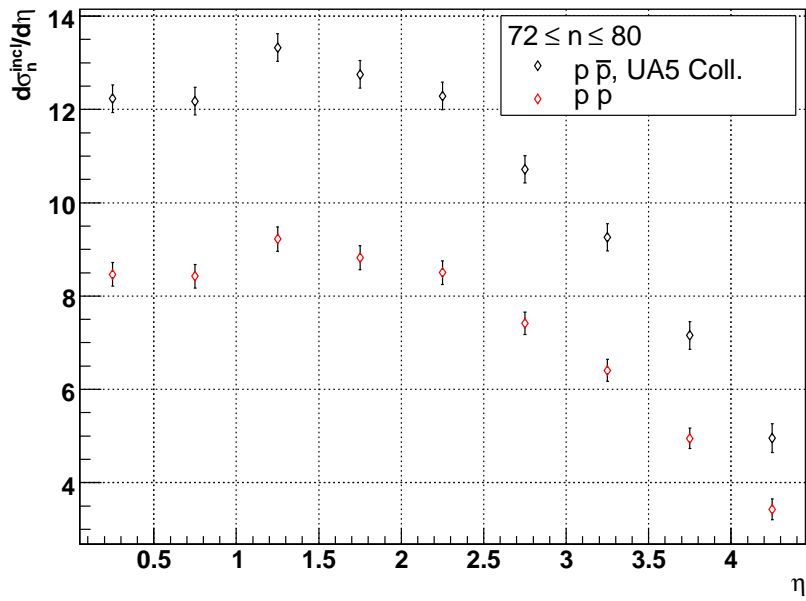


Figure 12: Inclusive pseudorapidity distributions for $72 \leq n \leq 80$

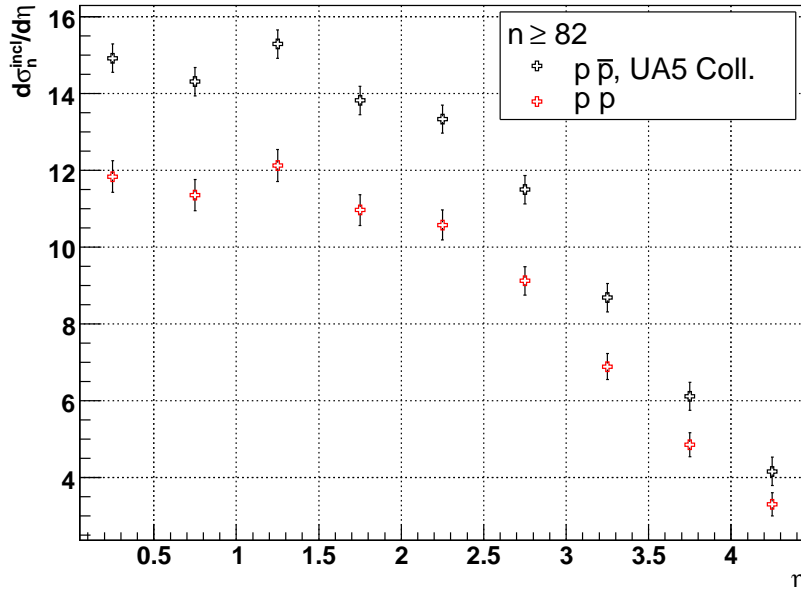


Figure 13: Inclusive pseudorapidity distributions for $n \geq 82$

References

- [1] UA5 Coll., R.E. Ansorge et al., Z. Phys. C **43** (1989) 357
- [2] UA5 Coll., G.J. Alner et al., Z. Phys. C **33** (1986) 1
- [3] ALICE Coll., K. Aamodt et al., arXiv:0911.5430v2 [hep-ex] (2009)
- [4] V.A. Abramovsky, O.V. Kancheli, Pisma Zh. Eksp. Teor. Fiz. **15** (1972) 559
- [5] V.A. Abramovsky, V.N. Gribov, O.V. Kancheli, Yad. Fiz. **18** (1973) 595
- [6] A.B. Kaidalov, K.A. Ter-Martirosyan, Yad. Fiz. **39** (1984) 1545
- [7] A. Capella, U. Sukhatme, C.-I. Tan and J. Tran Tha Van, Phys. Rep **40** (1984) 211
- [8] V.A. Abramovsky, N.V. Radchenko, Particles and Nuclei, Letters **6** (2009) 607
- [9] V.A. Abramovsky, N.V. Radchenko, Particles and Nuclei, Letters **6** (2009) 717
- [10] V.A. Abramovsky, N.V. Radchenko, arXiv:0812.2465v1 [hep-ph] (2008)
- [11] N.V. Radchenko, arXiv:0911.4847v1 [hep-ph] (2009)
- [12] V.A. Abramovsky, arXiv:0911.4850v1 [hep-ph] (2009)
- [13] V.A. Abramovsky, O.V. Kancheli, Pisma Zh.Eksp.Teor.Fiz. **31** (1980) 566 and Pisma Zh.Eksp.Teor.Fiz. **32** (1980) 498